Workshop on Virtual Reality Interaction and Physical Simulation VRIPHYS (2015)
F. Jaillet, G. Zachmann, and F. Zara (Editors)

Supplementary Material: Evaluation of Surface Tension Models for SPH-Based Fluid Animations Using a Benchmark Test

Markus Huber[1], Stefan Reinhardt[2], Daniel Weiskopf[1], and Bernhard Eberhardt[2]

[1]VISUS, University of Stuttgart, Germany [2]Stuttgart Media University, Germany

1. Overview

In this document, we provide additional images and plots to the main paper. First, images of the equilibrium state of benchmark 1 (drop formation) are shown for all surface tension models presented in Sec. 3 in the main paper, combined with different SPH methods (IISPH [ICS*14], PCISPH [SP09], and WCSPH [BT07]). Further, individual plots for velocities, surface tension forces, and pressure forces that are shown as aggregated values in Sec. 6 of the main paper, are given. At last, velocity plots for benchmark 2 (liquid crown) applied to the mentioned surface tension models in combination with IISPH and WCSPH are given.

2. Drop Formation

2.1. Using IISPH

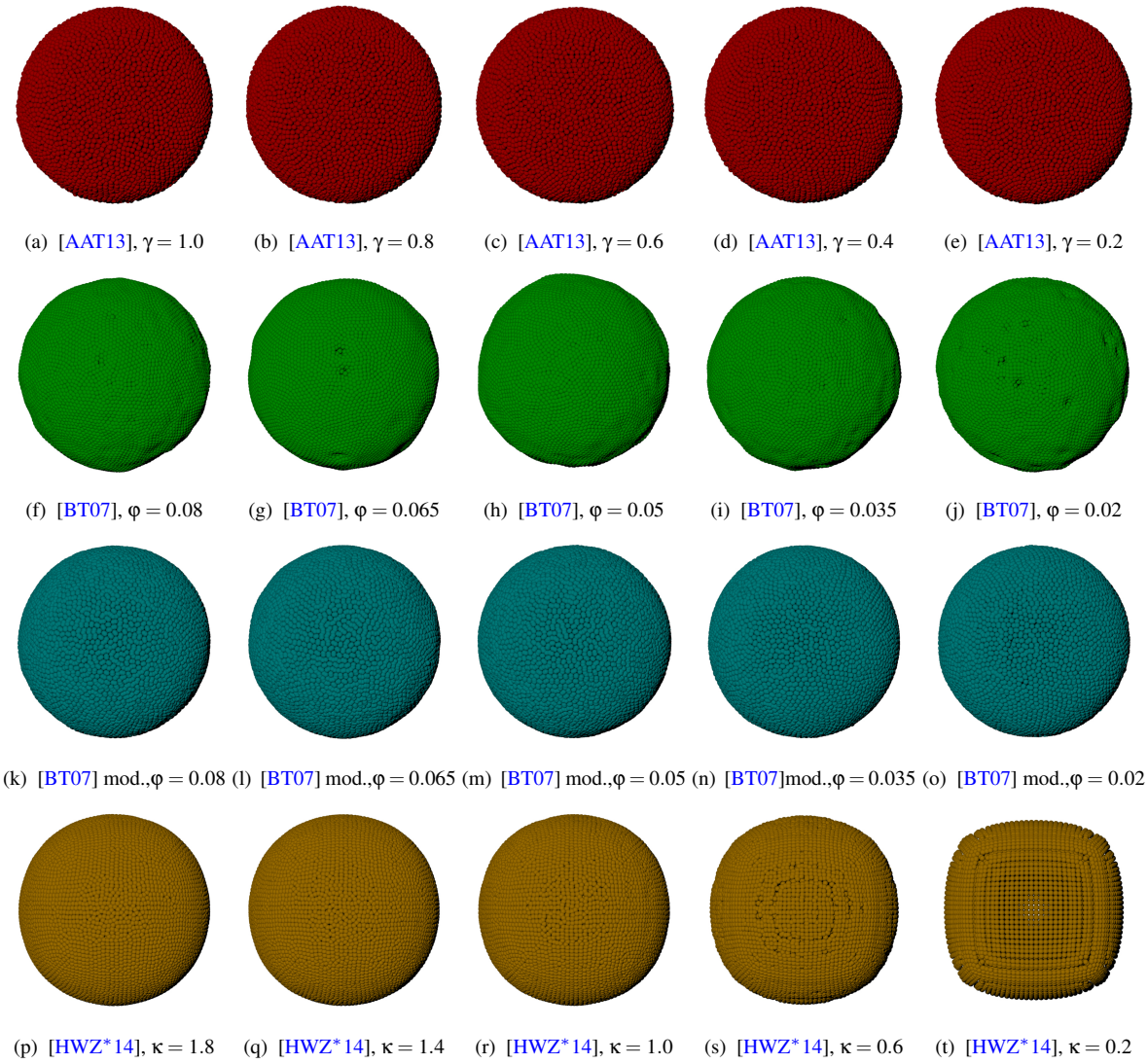

(a) [AAT13], $\gamma = 1.0$ (b) [AAT13], $\gamma = 0.8$ (c) [AAT13], $\gamma = 0.6$ (d) [AAT13], $\gamma = 0.4$ (e) [AAT13], $\gamma = 0.2$

(f) [BT07], $\varphi = 0.08$ (g) [BT07], $\varphi = 0.065$ (h) [BT07], $\varphi = 0.05$ (i) [BT07], $\varphi = 0.035$ (j) [BT07], $\varphi = 0.02$

(k) [BT07] mod.,$\varphi = 0.08$ (l) [BT07] mod.,$\varphi = 0.065$ (m) [BT07] mod.,$\varphi = 0.05$ (n) [BT07]mod.,$\varphi = 0.035$ (o) [BT07] mod.,$\varphi = 0.02$

(p) [HWZ*14], $\kappa = 1.8$ (q) [HWZ*14], $\kappa = 1.4$ (r) [HWZ*14], $\kappa = 1.0$ (s) [HWZ*14], $\kappa = 0.6$ (t) [HWZ*14], $\kappa = 0.2$

Figure 1: Snapshots of the equilibrium state of benchmark 1 (drop formation) applied to all surface tension models in combination with IISPH. Except for low surface tension coefficients with the model of He et al. [HWZ*14], a spherical shape is achieved with all combinations of models. With the surface tension model of Becker and Teschner [BT07], deformations of the sphere occur that are resolved with our modifications.

2.2. Using PCISPH

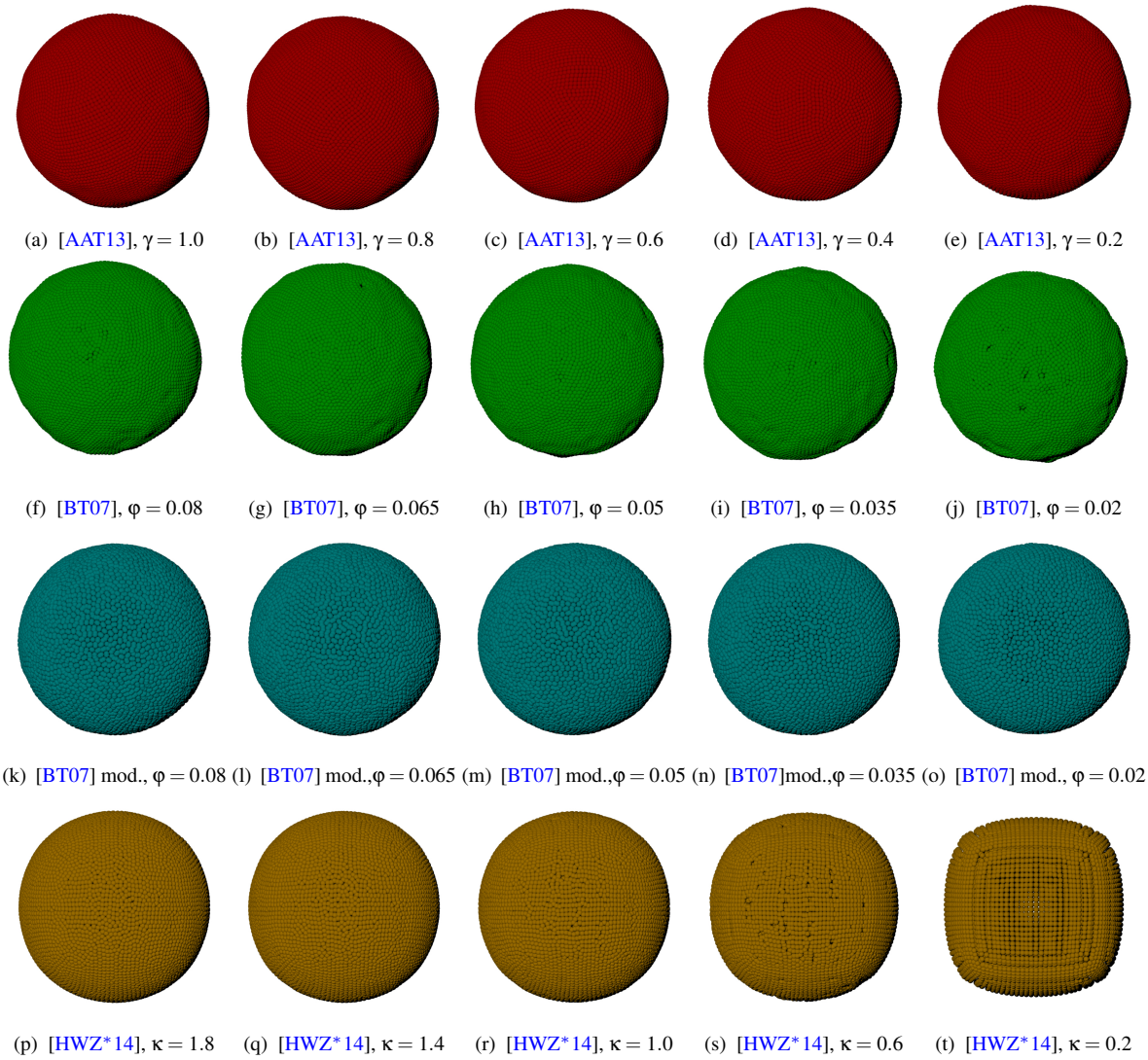

(a) [AAT13], $\gamma = 1.0$ (b) [AAT13], $\gamma = 0.8$ (c) [AAT13], $\gamma = 0.6$ (d) [AAT13], $\gamma = 0.4$ (e) [AAT13], $\gamma = 0.2$

(f) [BT07], $\varphi = 0.08$ (g) [BT07], $\varphi = 0.065$ (h) [BT07], $\varphi = 0.05$ (i) [BT07], $\varphi = 0.035$ (j) [BT07], $\varphi = 0.02$

(k) [BT07] mod., $\varphi = 0.08$ (l) [BT07] mod.,$\varphi = 0.065$ (m) [BT07] mod.,$\varphi = 0.05$ (n) [BT07]mod.,$\varphi = 0.035$ (o) [BT07] mod., $\varphi = 0.02$

(p) [HWZ*14], $\kappa = 1.8$ (q) [HWZ*14], $\kappa = 1.4$ (r) [HWZ*14], $\kappa = 1.0$ (s) [HWZ*14], $\kappa = 0.6$ (t) [HWZ*14], $\kappa = 0.2$

Figure 2: Snapshots of the equilibrium state of benchmark 1 (drop formation) applied to all surface tension models in combination with PCISPH. Similar results to the previous combination (using IISPH) are achieved.

2.3. Using WCSPH

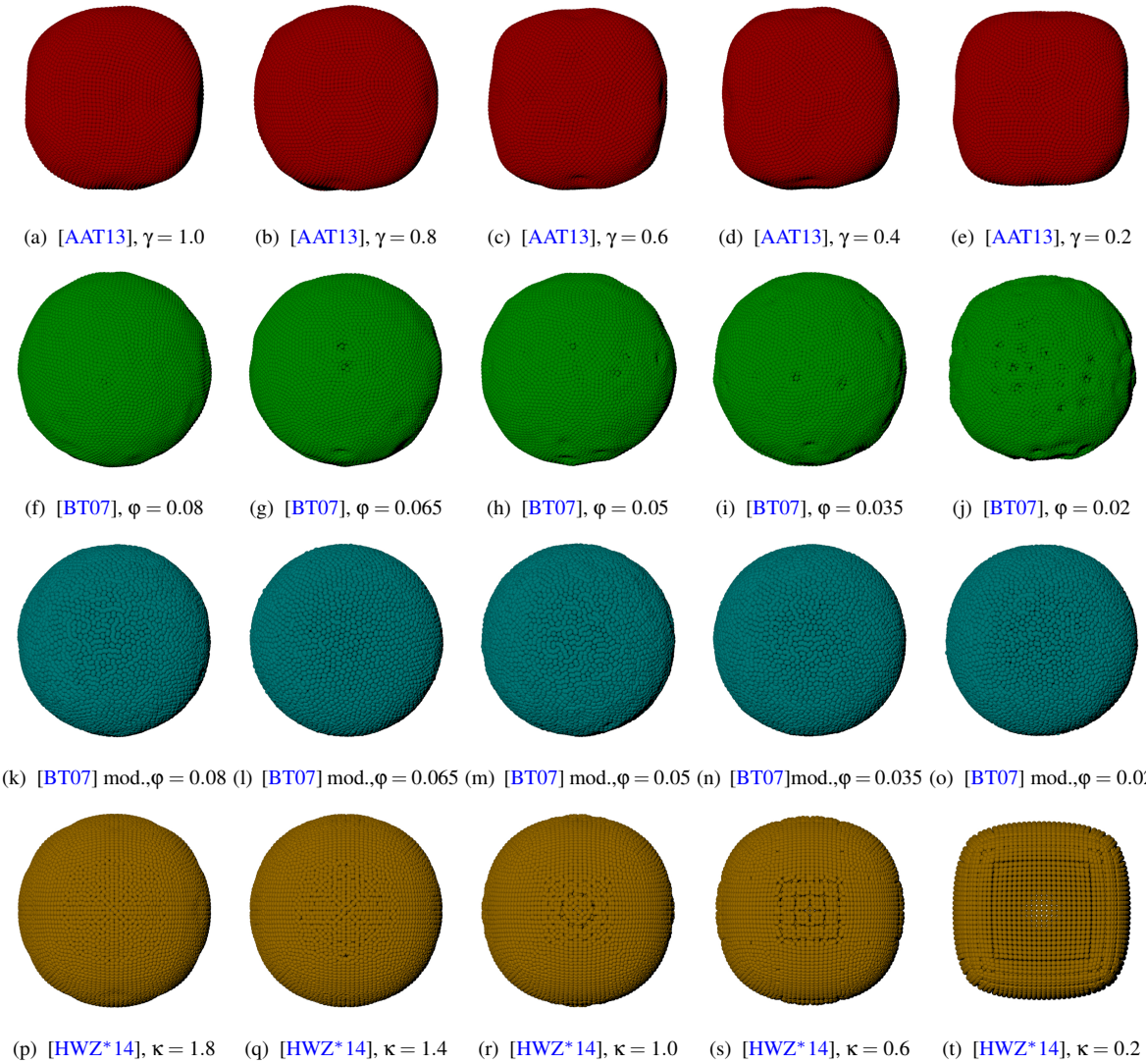

(a) [AAT13], $\gamma = 1.0$ (b) [AAT13], $\gamma = 0.8$ (c) [AAT13], $\gamma = 0.6$ (d) [AAT13], $\gamma = 0.4$ (e) [AAT13], $\gamma = 0.2$

(f) [BT07], $\varphi = 0.08$ (g) [BT07], $\varphi = 0.065$ (h) [BT07], $\varphi = 0.05$ (i) [BT07], $\varphi = 0.035$ (j) [BT07], $\varphi = 0.02$

(k) [BT07] mod.,$\varphi = 0.08$ (l) [BT07] mod.,$\varphi = 0.065$ (m) [BT07] mod.,$\varphi = 0.05$ (n) [BT07]mod.,$\varphi = 0.035$ (o) [BT07] mod.,$\varphi = 0.02$

(p) [HWZ*14], $\kappa = 1.8$ (q) [HWZ*14], $\kappa = 1.4$ (r) [HWZ*14], $\kappa = 1.0$ (s) [HWZ*14], $\kappa = 0.6$ (t) [HWZ*14], $\kappa = 0.2$

Figure 3: Snapshots of the equilibrium state of benchmark 1 (drop formation) applied to all surface tension models in combination with WCSPH. With very low values for the surface tension coefficient, no spherical shape is formed. The results achieved with the model of He et al. [HWZ*14] shows almost no difference in combination with different SPH methods.

3. Measurements Benchmark Test 1 (Drop Formation)

3.1. Velocities

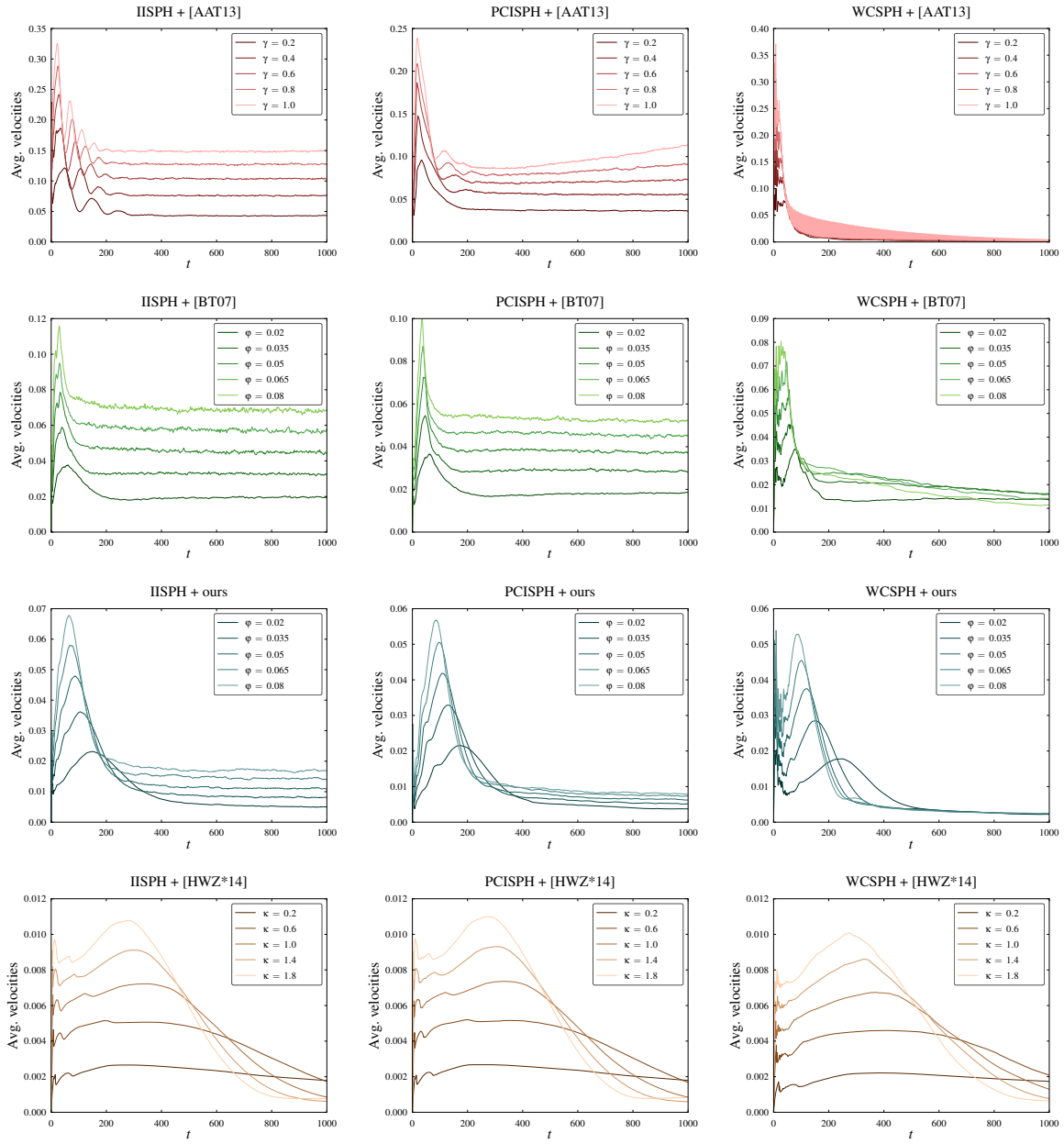

Figure 4: Temporal plots of average particle velocities of all combinations of surface tension models with different SPH models for benchmark test 1 (drop formation). Velocities are given in $\frac{m}{s}$ and time t is given in s. With the surface tension model by Akinci et al. [AAT13], initial oscillations can be recognized in the local extreme values in the velocities, especially in combination with IISPH. With the models by Becker and Teschner [BT07] and He et al. [HWZ*14], velocities in the equilibrium state are much lower than with the model of Akinci et al. With the method of He et al., the equilibrium state is reached considerably later than with the other models. As observed in the animations, the overall behaviour of the velocity using the model of He et al. is only little affected by the used SPH simulation model.

3.2. Surface tension forces

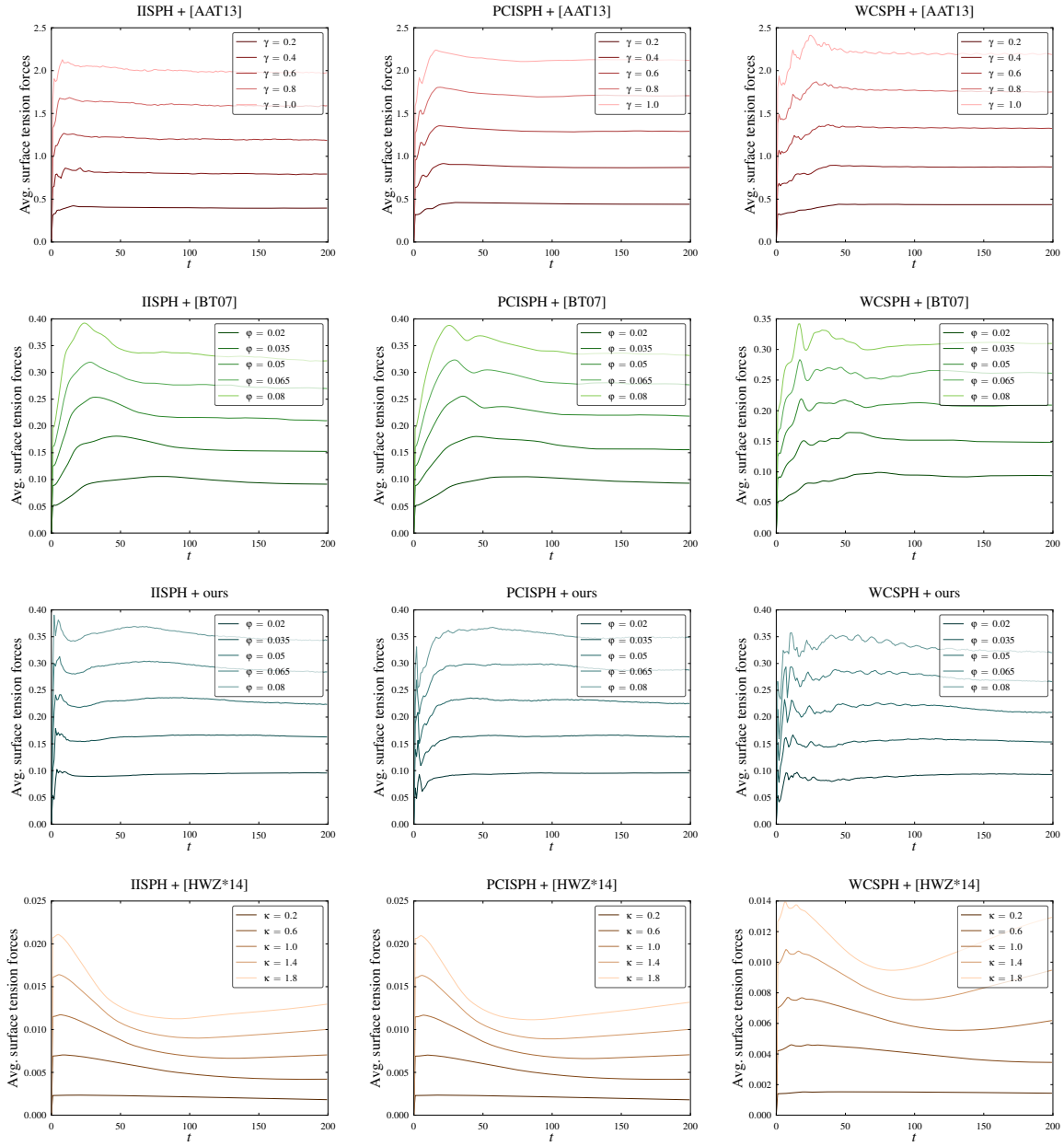

Figure 5: Temporal plots of average surface tension forces of all combinations of surface tension models with different SPH models for benchmark test 1 (drop formation). Surface tension forces are given in N and time t is given in s. The equilibrium state of surface tension forces is reached considerably earlier than the respective velocities. Hence, the plots cover 200 frames as opposed to 1000 with the velocities to see all the details in oscillations.

3.3. Pressure forces

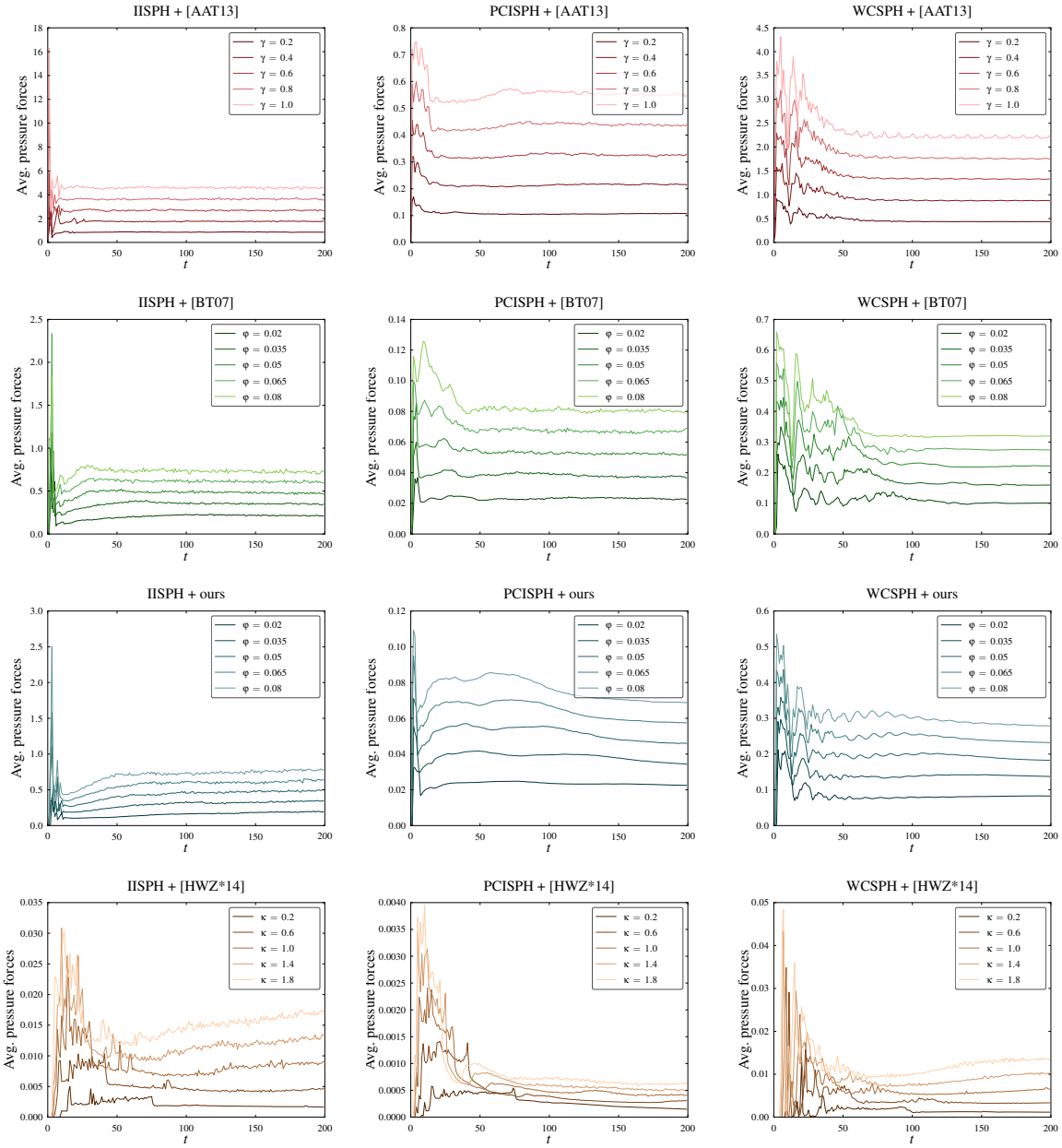

Figure 6: Temporal plots of average pressure forces of all combinations of surface tension models with different SPH models for benchmark test 1 (drop formation). Pressure forces are given in N and time t is given in s. The equilibrium state of pressure forces is also reached earlier than the respective velocities. Hence, the plots cover 200 frames as opposed to 1000 with the velocities to see all the details in oscillations.

4. Measurements Benchmark Test 2 (Liquid Crown)

4.1. Velocities

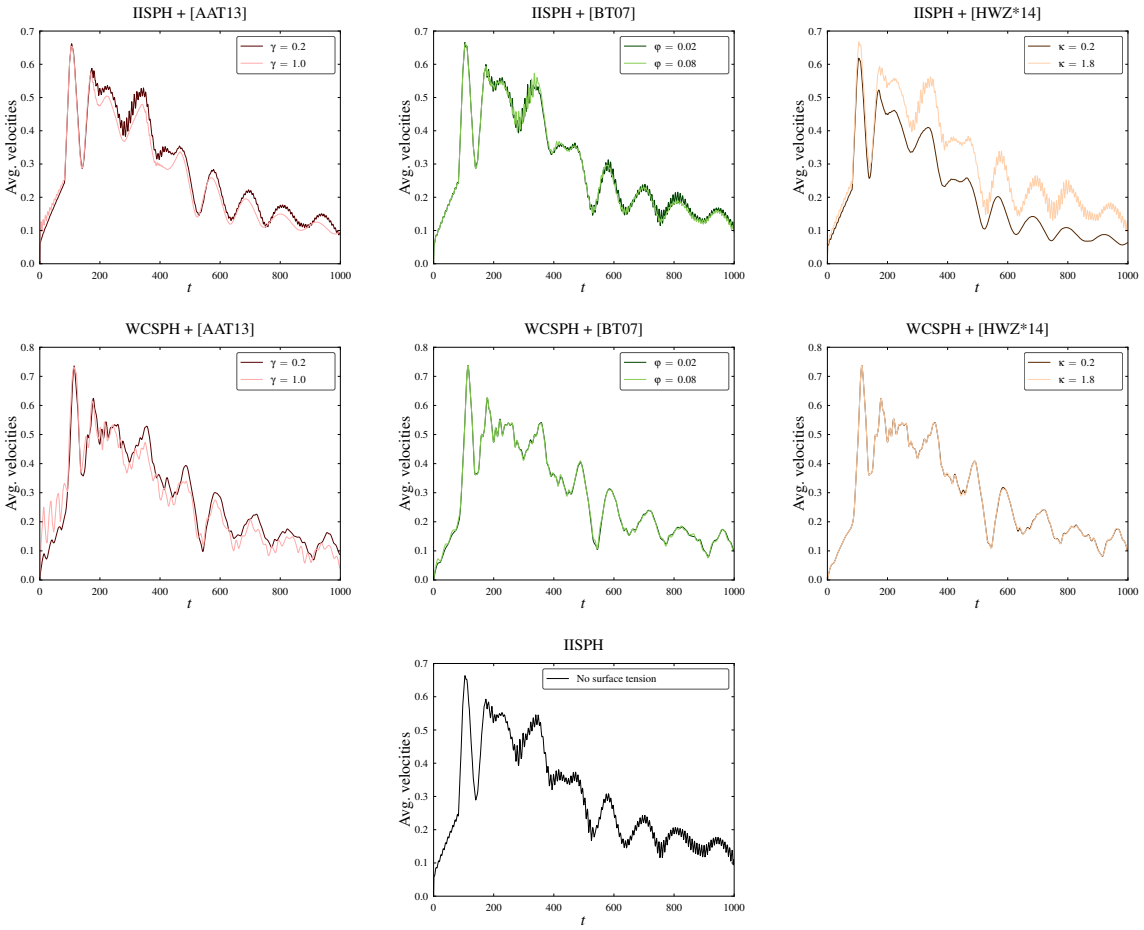

Figure 7: Temporal plots of average particle velocities for a set of combination of surface tension models with SPH models for benchmark test 2 (liquid crown). Only small differences can be noticed using varying surface tension parameters. However, there are big differences in the resulting animations (see main paper and accompanying video).

References

[AAT13] AKINCI N., AKINCI G., TESCHNER M.: Versatile surface tension and adhesion for SPH fluids. *ACM Transactions on Graphics 32*, 6 (2013), 182:1–182:8. doi:10.1145/2508363.2508395. 2, 3, 4, 5

[BT07] BECKER M., TESCHNER M.: Weakly compressible SPH for free surface flows. In *ACM SIGGRAPH/Eurographics Symposium on Computer Animation* (2007), pp. 209–218. doi:10.2312/SCA/SCA07/209-218. 1, 2, 3, 4, 5

[HWZ*14] HE X., WANG H., ZHANG F., WANG H., WANG G., ZHOU K.: Robust simulation of sparsely sampled thin features in SPH-based free surface flows. *ACM Transactions on Graphics 34*, 1 (2014), 7:1–7:9. doi:10.1145/2682630. 2, 3, 4, 5

[ICS*14] IHMSEN M., CORNELIS J., SOLENTHALER B., HORVATH C., TESCHNER M.: Implicit incompressible SPH. *IEEE Transactions on Visualization and Computer Graphics 20*, 3 (2014), 426–435. doi:10.1109/TVCG.2013.105. 1

[SP09] SOLENTHALER B., PAJAROLA R.: Predictive-corrective incompressible SPH. *ACM Transactions on Graphics 28*, 3 (2009), 40:1–40:6. doi:10.1145/1531326.1531346. 1